Carbon Onions: Carriers of the 217.5 nm Interstellar Absorption Feature

Manish Chhowalla,[1] H. Wang,[2] N. Sano,[3] K. B. K. Teo,[2] S. B. Lee,[4] and G. A. J. Amaratunga[2]

[1]*Rutgers University, Ceramic and Materials Engineering, Piscataway, New Jersey 08854*
[2]*Cambridge University, Engineering Department, Trumpington Street, Cambridge, United Kingdom*
[3]*Himeji Institute of Technology, Chemical Engineering Department, Himeji, Japan*
[4]*Department of Nanotechnology, Hanyang University, Seoul, Korea*

(Received 15 January 2003; published 16 April 2003)

Ultraviolet-visible absorption measurements of high purity and well separated carbon onion samples are reported. The results show that, after purification, absorption features from carbon onions match well with the interstellar UV spectrum. The measurements show that the absorption peak position remains constant at $4.55 \pm 0.1\ \mu m^{-1}$, and the width varies from 1.2–1.6 μm^{-1}, a key feature of the interstellar spectrum. The similarities between the experimental and observed absorption spectra indicate that carbon onions are very strong candidates for the origin of the UV interstellar absorption peak at $4.6\ \mu m^{-1}$.

DOI: 10.1103/PhysRevLett.90.155504 PACS numbers: 61.48.+c, 61.46.+w

Origin of the interstellar dust ultraviolet (UV) absorption spectrum with a constant peak position at 217.5 nm ($4.6\ \mu m^{-1}$, 5.7 eV) and width variation of up to 30% is unresolved [1–10]. Although carbonaceous dust particles are thought to be responsible for the astronomical feature, no conclusive evidence has been found to confirm this conjecture [7,10]. Theoretical studies have suggested that spherical concentric fullerenes referred to as carbon onions could be responsible [6,8,9] because their π-plasmon resonance energy (5.6 eV) closely corresponds to the interstellar absorption maximum. However, experimental results on carbon onions dispersed in water thus far show absorption spectra that are redshifted with the maximum centered at around $3.8\ \mu m^{-1}$ [7,10]. The redshift is generally attributed to the presence of the water medium as well as the inability to adequately prevent agglomeration of the carbon onions [8].

Experiments designed to simulate the chemistry conditions in an atmosphere of a carbon star led to the discovery of the C_{60} fullerene molecule by Kroto *et al.* [11]. However, the optical properties of the smaller C_{60} and C_{70} fullerenes do not correspond to the interstellar UV absorption spectrum. This famous interstellar spectrum was first measured in the 1960s [1,2] and the explanation, based on calculations, for its origin from the start was attributed to particles with properties similar to graphite. The quest to reproduce this astronomical feature in the laboratory by Kratschmer *et al.* [12] led to the production of macroscopic quantities of fullerenes, revolutionizing nanocarbon research. Pioneering experimental work on the absorption from polyhedral carbon onions was reported by de Heer and Ugarte [7]. They measured the UV absorption spectra of annealed carbon soot dispersed in water. Their results showed an extinction peak at $3.8\ \mu m^{-1}$. They suggested that the water environment and clustering effects [7,8] caused the redshift in their measured spectra in comparison to the interstellar absorption feature. Wada *et al.* on the other hand simulated mass ejection from stellar atmospheres in the laboratory using methane plasma to produce carbonaceous material containing onionlike particles that showed an absorption peak at $4.6\ \mu m^{-1}$ [13]. However, their material is thought to contain other hydrocarbon materials as well as onionlike particles and therefore the absorption near $4.6\ \mu m^{-1}$ cannot be unequivocally be ascribed to onions.

After the discovery of the C_{60}, Kroto and Mackay suggested that onionlike hyperfullerenes consisting of concentric shells were possible and stable [14]. Subsequently, Ugarte showed that spherical carbon hyperfullerenes consisting of multiple shells could be formed by electron beam irradiation of carbon soot in a transmission electron microscope (TEM) [15]. Furthermore, carbon onions can be formed by heat treatment and electron beam irradiation of nanodiamond [16]. Diamondlike structures can also form by vapor-phase decomposition of hydrocarbon gases [17]. The close relationship between carbon onions and diamond has been further demonstrated by Banhart and Ajayan, who showed that diamond could be nucleated within the cores of large onions [18]. Indeed, nanodiamond and carbon onions have been observed via TEM in meteorites [19,20]. In addition, infrared peaks corresponding to sp^3 hybridization have been detected in the absorption spectra of dense interstellar clouds [21]. Therefore, the presence of diamond and hydrocarbon species in interstellar dust point to conditions which are favorable for the formation of carbon onions.

Here we report on experimental ultraviolet-visible (UV-VIS) absorption spectra from high purity, well-dispersed carbon onions that closely match the interstellar feature. The electron microscopy images of carbon onions used in this study are shown in Fig. 1. The carbon onions were prepared by striking an arc discharge between two graphite electrodes submerged in water or liquid nitrogen [22,23]. The onion thin films were prepared by dispersing the onions in water and

ultrasonicating (using IKA U50 probe) for 5 min in short 5 s pulses. The samples were dried in air and then annealed in air at 600 °C for 20–60 min. A UV-VIS spectrometer with a wavelength range of 188–900 nm was used. The reflection and transmission measurements were calibrated using a clean quartz disk prior to every measurement series for each sample.

A high magnification scanning electron microscopy (SEM) image of carbon onions dispersed on a highly conducting silicon surface are shown in Fig. 1(a). The onions are generally agglomerated as clusters on the substrate even after rigorous ultrasonic treatments. Higher magnification TEM observations generally reveal two types of carbon onions in our sample [22,23]. The size of the onions ranged from 3–50 nm, as can be seen from the TEM images in Figs. 1(b)–1(d).

The absorption spectra from dispersed carbon onion thin films on quartz disks before and after annealing are presented in Figs. 2(d)–2(f), respectively. Also shown in the figure are absorption spectra from polyhedral graphite [Fig. 2(a)], amorphous carbon [Fig. 2(b)], and the interstellar absorption feature [Fig. 2(c)]. The measured curves are the result of over 100 measurements on several different samples. The majority of the measured spectra prior to annealing were similar to those reported by de Heer and Ugarte with a maximum centered at around $4.0 \pm 0.1\ \mu\text{m}^{-1}$ and widths (γ) ranging from 2.0–3.5 μm^{-1}. The very large width values in some of the measured spectra prior to annealing are attributed to the presence of amorphous carbon and polyhedral graphite contaminants in the carbon onion thin films. Digital camera images shown in the inset of Fig. 2 show that the carbon onion thin film on quartz is almost completely transparent subsequent to the annealing treatment [Fig. 2(h)], in contrast to its opaque appearance prior to annealing [Fig. 2(g)]. Furthermore, Raman spectroscopy of the onion thin film prior to annealing (Fig. 3) shows the presence of a strong and broad "*D*" peak near 1350 cm^{-1},

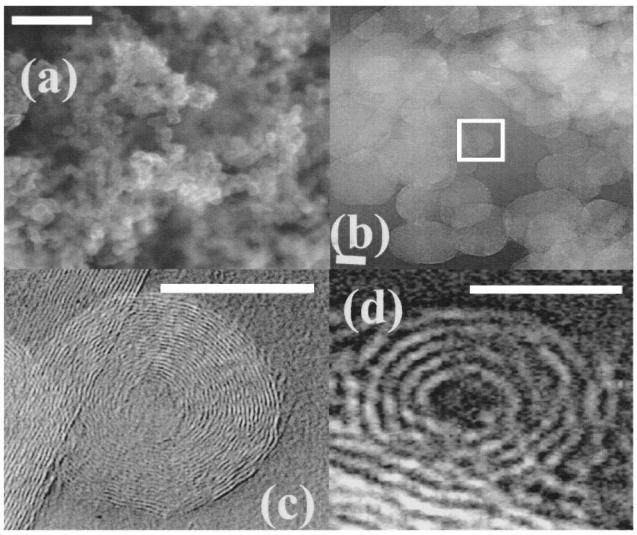

FIG. 1. (a) SEM image of dispersed carbon onion thin films on highly conducting silicon chip (scale bar = 300 nm), obtained using Hitachi S800-FR SEM operated at 20 kV. The high-resolution transmission electron microscopy (HREM) was performed on a JEOL 2010FX microscope operated at 200 kV. The TEM specimens were prepared by sprinkling the unpurified material onto a holey carbon grid. (b) A low magnification TEM image of carbon onions (scale bar = 20 nm). Enlarged high-resolution images of (c) ~17 nm (scale bar = 10 nm) and (d) ~5 nm (scale bar = 2.7 nm) diameter carbon onions.

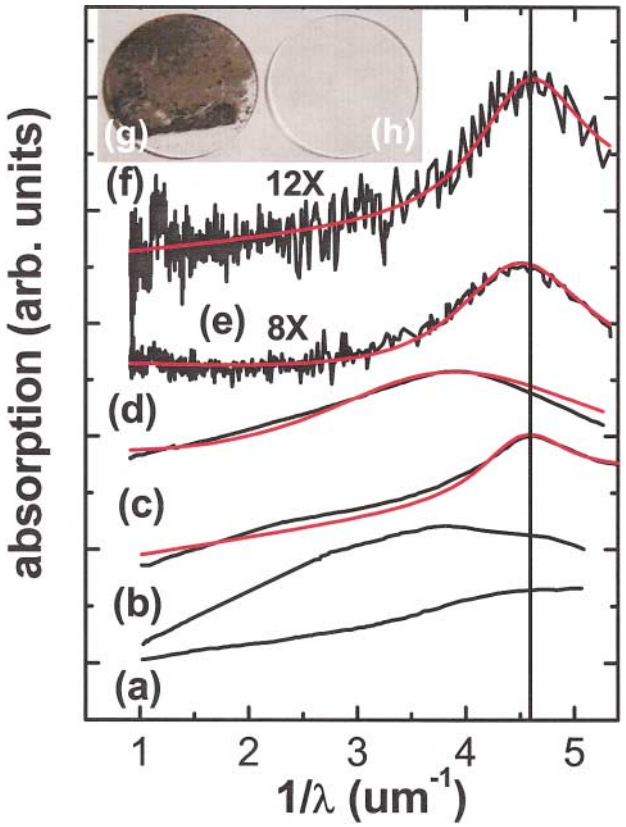

FIG. 2 (color). Absorption spectra of different carbonaceous materials as well as the interstellar absorption spectrum. The vertical line represents 4.6 μm^{-1}. Curve (*a*) is a spectrum from polyhedral graphite powder (Sigma Aldrich, particle size = 1–2 μm). Curve (*b*) is a typical spectrum of carbon soot scraped from graphite electrodes. Curve (*c*) is the interstellar absorption feature taken from Ref. [24]. Curve (*d*) is a typical spectrum obtained from our carbon onion thin films prior to annealing and compares well with other reports in the literature [7]. Curve (*e*) is an absorption spectrum from carbon onions with a width of 1.5 μm^{-1}, correlating well with the astronomical feature. Curve (*f*) is an absorption spectrum from carbon onions with a width of 1.2 μm^{-1}, in excellent agreement with the interstellar curve. The red curves in (*c*) (peak position = 4.6 μm^{-1}), (*d*) (peak position = 4.0 μm^{-1}), (*e*) (peak position = 4.55 μm^{-1}), and (*f*) (peak position = 4.6 μm^{-1}) represent the Drude function [24], used to obtain the peak position and width of the measured data.

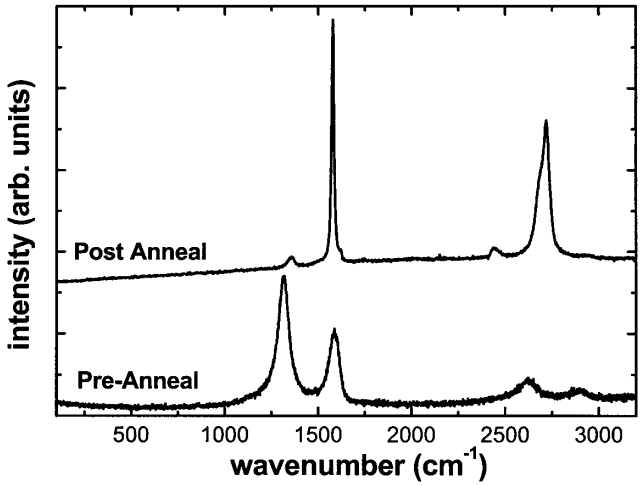

FIG. 3. Raman spectra of carbon onion thin films prior to annealing and subsequent to annealing at 600 °C in air for 30 min. The Raman was carried out using a Renishaw Micro Raman RM 1000 system with a spectral resolution of 4–6 cm^{-1}. A 514.5 nm Ar ion laser was used as the excitation source.

indicating the presence of microcrystalline graphite and amorphous carbon. The slightly higher absorption peak position in the unannealed carbon thin films can be attributed to the different dielectric constant of the surrounding medium in this case. The surface plasmon resonance energy thought to be responsible for the astronomical feature is generally affected by the dielectric constant of the medium. Therefore when the medium is changed from water (dielectric constant = 1.7) to air/vacuum (dielectric constant = 1), the surface plasmon energy is expected to shift to a higher energy.

In an attempt to eliminate amorphous and graphitic carbon from our onion thin films, we annealed the samples in air at 600 °C for 20–60 min. The dramatic change in the appearance of the thin film (inset of Fig. 2) was also accompanied by a change in its phonon characteristics. The Raman spectra from the annealed samples (see Fig. 3) showed only a minor "*D*" peak with a very sharp "*G*" peak, indicating the presence of a highly ordered nanocrystalline graphitic material. The absence of a strong *D* peak and the sharpness of the *G* peak in the Raman spectra indicate that most of the amorphous carbon and polyhedral microcrystalline graphite has been removed during the annealing process. The remaining transparent thin film on quartz after annealing was examined using atomic force microscopy (AFM). AFM observations shown in Fig. 4 reveal nanoparticles with an aspect ratio of ~1 ranging in size from 5–50 nm along with larger agglomerated particles that are hundreds of nanometers in diameter. Note that we did not find any elongated structures, such as those that would be expected from nanotubes, during our AFM investigation. Furthermore, we have confirmed the presence of onions after annealing

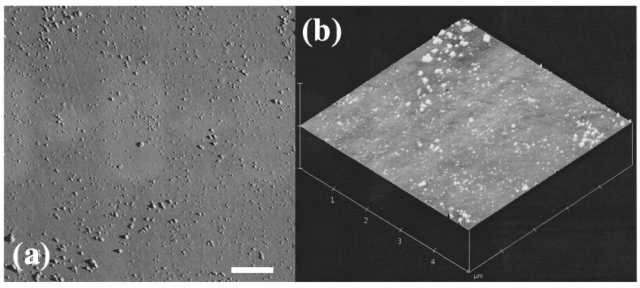

FIG. 4. AFM images of onion particles subsequent to annealing. A Digital Instrument's Nanoscope AFM was used in tapping mode at 0.3 Hz. The image is 512 pixels by 512 pixels. Most of the small particles are 20 nm in height and diameter and evenly distributed throughout the sample. The particles in the image appear pyramidal because their overall dimension is smaller than the AFM tip diameter. The scale bar is 1 μm.

through TEM. Their appearance was similar to those shown in Fig. 1, indicating that they survive the annealing treatment without damage. The absorption features of the annealed samples were also found to be dramatically different. A typical spectrum from a sample annealed at 600 °C for 30 min is shown in Fig. 2(e). The spectra from samples annealed for 30 min fit well with the interstellar UV absorption spectrum with the peaks centered at around $4.55 \pm 0.1\ \mu m^{-1}$ and variable widths ranging from 1.5–2.5 μm^{-1}. The observed widths of the samples annealed for 30 min are higher than those measured for the astronomical feature ($\gamma = 0.8$–$1.25\ \mu m^{-1}$). The higher widths in measurements here may arise from the fairly large size distributions of onions in our samples as well as remnant amorphous carbon. In an attempt to further decrease the width of the measured absorption spectrum, we annealed the samples at varying times, ranging from 20 min to 24 h. We found that widths as low as $1.2\ \mu m^{-1}$ can be measured for samples annealed in air at 600 °C for 1 h, as shown in Fig. 2(f). For samples annealed in air at 600 °C, the widths were found to vary from 1.2 to $1.6\ \mu m^{-1}$. The substantial decrease in the widths for samples annealed for 1 h is attributed to the elimination of amorphous carbon. Longer annealing times did not decrease the width dramatically and after several hours of annealing, the width was observed to increase. The fact that the peak position measured in our annealed samples is independent of the width variation is a strong indication that the spectra correlate to the interstellar feature and are not due to anomalies. Indeed, infrared analysis using FTIR did not reveal any C-H, O-H, or N-H stretching bands subsequent to annealing, indicating that the sample is free of such contaminants.

Theoretical work has suggested that the dielectric properties of closed carbon structures differ from bulk properties of graphite [25]. We have investigated the dielectric characteristics of carbon onions and polycrystalline graphite by measuring the low loss features in the

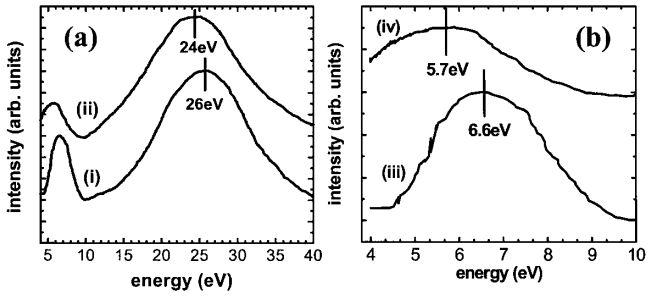

FIG. 5. (a) Low loss region of EELS for (i) polycrystalline graphite and (ii) carbon onions. The EELS was performed on a Phillips CM30 TEM operated at 100 kV equipped with a Gatan 666 spectrometer with a collection semiangle of 0.5 mrad. The energy resolution was 0.7 eV. The zero loss peak has been removed for clarity. (b) Enlarged π-plasmon energy region shown in greater detail. The π plasmon of (iii) graphite is centered at 6.6 eV while the maximum of the (iv) carbon onion π plasmon is located at 5.7 eV (4.6 μm^{-1}), correlating to the interstellar absorption maximum. The data shown here are an average of 15 measurements.

electron energy loss spectra (EELS). The low loss EELS spectra for graphite and carbon onions are shown in Fig. 5. The broad peaks at higher energies represent the plasmon energy from collective excitation of both σ and π valence electrons. However, the more important result is the position of the low energy peaks in Fig. 5 that arise from the collective plasmon excitation of the π electrons. It can be seen from Fig. 5(b) that the π plasmon for the carbon onions is centered at 5.7 eV (4.6 μm^{-1}) compared to 6.6 eV for graphite. Our results are in excellent agreement with the results of Cabioch *et al.*, who measured plasmon excitation energies using transmission and reflection EELS on their carbon onions [26]. The EELS results clearly confirm that π plasmons in carbon onions correlate with the maximum in the UV interstellar absorption spectrum.

There is evidence that carbon onions can form in interstellar space [21]. Here we discuss the origin of interstellarlike absorption spectra in our carbon onion samples. Although the SEM observation of the carbon onion thin films revealed mostly agglomerates [Fig. 1(a)], regions of well separated (i.e., unclustered) onions are clearly visible in the post annealed AFM images (Fig. 4). Previous absorption studies of carbon onions have been hampered by the inability to synthesize unclustered samples. We believe that it is these regions that give rise to the interstellarlike absorption spectra. The lack of damping due to clustering and the collective plasmon resonance of individual carbon onions in well-dispersed areas are most likely reasons for the UV absorption features seen in Figs. 2(e) and 2(f) [8]. This hypothesis is supported by the low intensities of the absorption curves 2(e) and 2(f), an indication that they have been measured from a very thin or well-dispersed region.

In conclusion, the UV-VIS characteristics of carbon onions fabricated by an arc discharge in water or liquid nitrogen show characteristics that are similar to the interstellar absorption feature. High purity and well separated carbon onion samples prepared by annealing the as-fabricated powder in air at 600 °C for 60 min show a constant absorption peak at 4.6 μm^{-1} with a variable width ranging from 1.2–1.6 μm^{-1}. In addition to the UV-VIS data, we confirm that the origin of the absorption feature at 4.6 μm^{-1} in carbon onions can be attributed to the collective excitations of π plasmons.

We thank Dr. Daping Chu for help with AFM measurements. We thank Dr. Satoshi Tomita for getting us interested in absorption from onions. M. C. acknowledges support from the Royal Academy of Engineering, U.K.

[1] T. P. Stecher and B. Donn, Astrophys. J. **142**, 1681 (1965).
[2] T. Stecher, Astrophys. J. **157**, L125 (1969).
[3] E. M. Purcell and C. R. Pennypacker, Astrophys. J. **186**, 705 (1973).
[4] K. L. Day and D. R. Huffman, Phys. Sci. **243**, 50 (1973).
[5] B. T. Dmine and H. M. Lee, Astrophys. J. **285**, 89–108 (1984).
[6] E. L. Wright, Nature (London) **336**, 227–228 (1988).
[7] W. A. de Heer and D. Ugarte, Chem. Phys. Lett. **207**, 480–486 (1993).
[8] A. A. Lucas *et al.*, Phys. Rev. B **44**, 2888–2896 (1994).
[9] L. Henrard *et al.*, Astrophys. J. **487**, 719–727 (1997).
[10] S. Tomita *et al.*, Phys. Solid State **44**, 450–453 (2002).
[11] H. W. Kroto *et al.*, Nature (London) **318**, 162–163 (1985).
[12] W. Kratschmer *et al.*, Nature (London) **347**, 354–358 (1990).
[13] S. Wada *et al.*, Astron. Astrophys. **345**, 259–264 (1999).
[14] H.W. Kroto and K. Mackay, Nature (London) **331**, 328–331 (1988).
[15] D. Ugarte, Nature (London) **359**, 707–709 (1992).
[16] V. L. Kuznetsov *et al.*, Chem. Phys. Lett. **222**, 343–348 (1994).
[17] J. C. Angus and C. C. Hayman, Science **241**, 913–921 (1988).
[18] F. Banhart and P. M. Ajayan, Nature (London) **382**, 433–435 (1996).
[19] P. P. K. Smith and P. R. Buseck, Science **212**, 322–324 (1981).
[20] T. J. Bernatowicz *et al.*, Astrophys. J. **472**, 760 (1996).
[21] L. J. Allamandola *et al.*, Science **260**, 64–66 (1993).
[22] N. Sano *et al.*, Nature (London) **414**, 506–507 (2001).
[23] N. Sano *et al.*, J. Appl. Phys. **92**, 2783–2788 (2002).
[24] E. L. Fitzpartick and D. Massa, Astrophys. J. **307**, 286–294 (1986).
[25] M. S. Dresselhaus, G. Dresselhaus, and P. C. Eklund, *Science of Fullerenes and Carbon Nanotubes* (Academic Press, New York, N.Y., 1996).
[26] T. Cabioc'h *et al.*, Europhys. Lett. **38**, 471–475 (1997).